



Systemic ventricular strain and torsion are predictive of elevated serum NT-proBNP in Fontan patients: a magnetic resonance study

Li-Wei Hu^{1#}, Xin-Rong Liu^{2#}, Qian Wang¹, Gregory P. Barton^{3,4}, Rong-Zhen Ouyang¹, Ai-Min Sun¹, Chen Guo¹, Tong-Tong Han⁵, Xiao-Fen Yao¹, Christopher J. François³, Yu-Min Zhong¹

¹Diagnostic Imaging Center, ²Department of Cardiothoracic Surgery, Shanghai Children's Medical Center Affiliated with Shanghai Jiao Tong University School of Medicine, Shanghai 200127, China; ³Department of Radiology, ⁴Department of Pediatrics and Medicine, University of Wisconsin-Madison, Madison, Wisconsin, USA; ⁵Circle Cardiovascular Imaging, Calgary, Alberta, Canada

#These authors contributed equally to this work.

Correspondence to: Yu-Min Zhong, MD, PhD. Diagnostic Imaging Center, Shanghai Children's Medical Center Affiliated with Shanghai Jiao Tong University School of Medicine, No.1678 Dong Fang Road, Shanghai 200127, China. Email: zyumin2002@163.com; Christopher J. François, MD. Department of Radiology, University of Wisconsin-Madison, 1111 Highland Ave., Madison, WI, USA. Email: cfrancois@uwhealth.org.

Background: This study aimed to investigate the associations between cardiac strain, cardiac torsion, ventricular volumes, and ventricular ejection fraction, with N-terminal pro-B-type natriuretic peptide (NT-proBNP) levels in Fontan patients who were age- and gender-matched with healthy control subjects.

Methods: Cardiovascular magnetic resonance (CMR) studies performed in 22 (15 male, 7 female) patients with single-ventricle physiology (all morphological left ventricles) palliated with Fontan and 17 (10 male, 7 female) age- and gender-matched healthy children volunteers were retrospectively analyzed. Serum NT-proBNP levels were obtained in Fontan subjects. Standard post-processing of CMR images included systemic ventricular end-diastolic and end-systolic volumes, stroke volume, cardiac mass, atrioventricular regurgitation, and ejection fraction. CMR tissue tracking (TT) software was used to quantify global longitudinal strain (GLS), global radial strain (GRS), and global circumferential strain (GCS) and torsion of the systemic ventricle. Pearson and Spearman correlation coefficients were used in comparisons of correlations between NT-proBNP and functional parameters in repair Fontan patients. Intra-observer and inter-observer variability of CMR strain and torsion values were determined from 10 randomly selected Fontan subjects and 10 randomly selected control subjects.

Results: GLS was significantly lower in Fontan patients than in control subjects (-15.19 ± 2.94 vs. -19.97 ± 1.70 ; $P < 0.001$). GLS was not significantly different between normal NT-proBNP levels and high NT-proBNP levels in Fontan patients (-15.59 ± 2.72 vs. -14.62 ± 3.32 ; $P = 0.462$). The GCS of repair Fontan patients was not significantly lower than that of the control group (-16.76 ± 3.27 vs. -17.88 ± 2.26 ; $P = 0.235$). GCS was significantly different between normal and high NT-proBNP levels group in Fontan patients (-17.95 ± 2.43 vs. -15.04 ± 3.67 ; $P = 0.036$). The peak systolic torsion and peak systolic torsion rates were significantly lower in Fontan patients than in control subjects (0.81 ± 0.41 vs. 1.07 ± 0.36 , $P = 0.044$; 7.36 ± 3.41 vs. 9.85 ± 2.61 , $P = 0.017$). Peak systolic torsion was significantly lower in Fontan patients with normal NT-proBNP levels than in high NT-proBNP subjects (0.67 ± 0.43 vs. 1.01 ± 0.29 ; $P = 0.036$). GCS and torsion were more strongly correlated with NT-proBNP in the patient group ($r = 0.541$ for GCS; $r = 0.588$ for torsion, $P < 0.01$). The parameters of strain and torsion could be reproduced with sufficient accuracy by intra-observer agreement (biases = 0.04 for GLS; biases = 0.66 for GCS; biases = 1.03 for GRS; biases = 0.04 for torsion) and inter-observer agreement (biases = 0.32 for GLS; biases = 0.85 for GCS; biases = 1.52 for GRS; biases = 0.18 for torsion).

Conclusions: GLS is an earlier marker of contractile dysfunction in repair Fontan patients. Peak systolic torsion may be a biomarker for determining subclinical dysfunction, as it is more strongly correlated with serum biomarkers of ventricular function than ventricular size or ejection fraction.

Keywords: Cardiovascular magnetic resonance (CMR); pediatric; torsion; Fontan; strain

Submitted Jun 27, 2019. Accepted for publication Jan 07, 2020.

doi: 10.21037/qims.2020.01.07

View this article at: <http://dx.doi.org/10.21037/qims.2020.01.07>

Introduction

Heart failure is a common complication in single-ventricle survivors with Fontan palliation that is a risk factor for mortality (1). N-terminal pro-B-type natriuretic peptide (NT-proBNP) is an important serum biomarker for pediatric patients with heart disease. In children with congenital heart disease (CHD), post-surgical NT-proBNP levels provide valuable prognostic information (2), with elevated levels strongly associated with the increased severity of ventricular systolic dysfunction (3).

Cardiovascular magnetic resonance (CMR) imaging is the reference standard for the quantification of ventricular volume and ejection fraction in Fontan patients (4). However, systemic ventricle ejection fraction (SVEF) reflects the geometric change of SV, but not the contractile function of the myocardium (5). Strain and torsion are alternative measures of myocardial deformation. Myocardial strain has been shown to be an earlier marker of contractile dysfunction than EF and may be well suited to revealing subclinical dysfunction in cardiac myocytes (6,7). Torsion is produced due to the double-helical nature of myocardial fibers, which results in systolic rotation in opposite directions between the apex and base of the ventricle in the longitudinal axis, which is a fundamental property of systolic function (8,9). Ventricular twist mechanics may provide a better understanding of the mechanisms of ventricular dysfunction (10).

However, there is little data on the relationship between perioperative NT-proBNP levels and CMR measures of ventricular function in patients with Fontan. Therefore, the purpose of this study was to investigate the associations between cardiac strain, cardiac torsion, ventricular volumes, and ventricular ejection fraction, with NT-proBNP levels in Fontan patients who were age- and gender-matched with healthy control subject. We hypothesized that the global ventricular strain and torsion would be changed in Fontan patients and be more strongly associated with NT-proBNP levels than standard volumetric measures of ventricular function.

Methods

Consecutive CMR studies performed between August 2014 and January 2019 in patients with Fontan were retrospectively identified according to a protocol approved by an institutional review board. Signed informed consent had been previously obtained before CMR for all participants. Subjects were included if serum NT-proBNP levels obtained within 1 month of the CMR study were also available. CMR studies in Fontan subjects were excluded if (I) they had undergone surgery within the last 6 months; (II) they had other diseases known to influence NT-proBNP levels, such as abnormalities in glomerular filtration, pulmonary hypertension, valvular stenosis (11); (III) they had had inadequate image quality for imaging analysis; or (IV) they had single-ventricle with the dominant morphology in the right ventricle (RV) (due to the difference in right and left ventricle mechanics). CMR studies performed in age- and sex-matched healthy volunteers without evidence of cardiovascular disease by echocardiography were included as control subjects.

CMR image acquisition

CMR was performed on a clinical 1.5 T scanner (Achieva, Philips Healthcare, Best, Netherlands) that included cine steady-state free precession (SSFP) short-axis views and two- and four-chamber views covering left ventricle. Acquisition parameters for the cine SSFP sequence were as follows: 3.1/1.5 ms repetition time/echo time; [288–320] × [288–320] acquisition matrix; 60° flip angle; 0 mm interslice gap; 6–7 mm slice thickness; 20–23 reconstructed phases per cardiac cycle.

CMR image analysis

All image post-processing was conducted with commercially available software (Version 5.9.1, Circle Cardiovascular Imaging, Calgary, AB, Canada). The left ventricle end-diastolic (EDVi) and end-systolic (ESVi) volumes, indexed

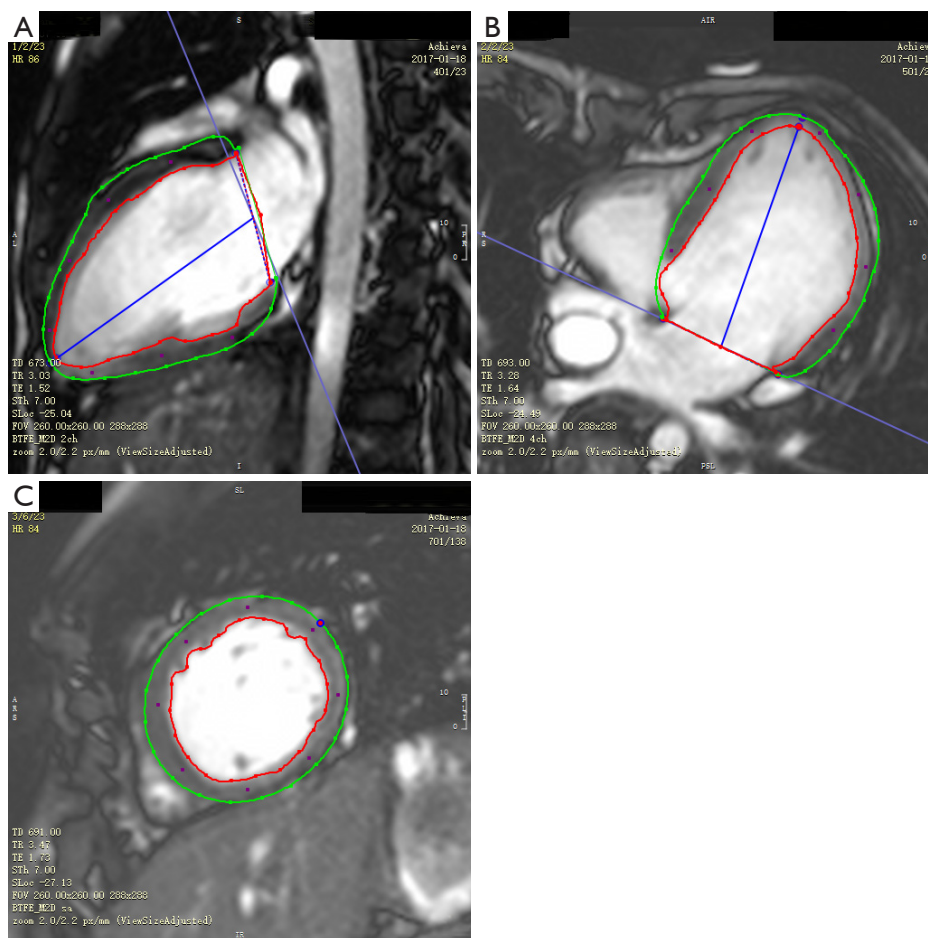


Figure 1 CMR tissue-tracking strain measurement in repaired Fontan patients using Circle CVI42 software. Only the morphological LV was included in the segmentation, and any residual hypoplastic right ventricle was excluded from the measurements. (A) cardiac 2-chamber view; (B) cardiac 4-chamber view; (C) cardiac short-axis view (green circle: epicardium; red circle: endocardium).

to body surface area, were obtained from short-axis cine SSFP images. Stroke volume index (SV_i) ejection fraction (EF) and cardiac output index (CO_i) were calculated from EDV and ESV. For Fontan patients, only the morphological LV was included in the segmentation, and any residual hypoplastic right ventricle was excluded from the measurements.

Myocardial strain and torsion of the LV were analyzed in Fontan patients. Tissue tracking (TT) analysis using the same software provided LV (A) global longitudinal (GLS), radial (GRS), and circumferential (GCS) strain; (B) torsion; and (C) torsion rate (12). Briefly, endocardial and epicardial contours were manually drawn on end-diastolic images for the short-axis and long-axis series. These end-diastolic contours were then automatically propagated to the other phases of the cardiac cycle (Figure 1). Global strain values

were derived from a 1D Lagrangian strain calculation. Torsion was defined as the basal clockwise rotation and apical clockwise rotation divided by the distance between apical and basal slices. Torsion rate was defined as the basal rotational velocity and apical clockwise rotational velocity divided by the distance between apical and basal slices.

Intra-observer and inter-observer variability of CMR strain and torsion measurements were determined from 10 randomly selected Fontan patients and 10 randomly selected control subjects.

Statistical analysis

Statistical analysis was performed using SPSS version 22.0 (IBM, Armonk, NY, USA). Continuous data are reported as mean ± standard deviation. Categorical data

Table 1 Characteristics of the Fontan patients

Variable	Patients (n=22)
CHD details	
Single left ventricle	10 (46%)
Tricuspid atresia	6 (27%)
Pulmonary atresia with intact ventricular septum	6 (27%)
Operative procedure	
Late tunnel Fontan	3 (14%)
Extracardiac Fontan	19 (86%)
Fenestrated	17 (77%)
Non-fenestrated	5 (23%)
Ventricular	
Complex 2 ventricles	12 (54%)
Single ventricle	10 (45%)
Aorta origin	
LV ventricle	18 (82%)
Hypoplastic right ventricle	4 (18%)
NYHA classification	
I	18 (82%)
II	4 (18%)
NT-ProBNP	
>125 pg/mL	9 (41%)
<125 pg/mL	13 (59%)

are reported as numbers with percentages. Comparisons between 2 groups were made using an independent Student's *t*-test for normally distributed data and Mann-Whitney U test for non-normally distributed continuous variables using GraphPad prism version 6.0. Pearson and Spearman correlation coefficients were used in comparisons of correlations between NT-proBNP and functional parameters (EDV, ESV, SV, EF, GLS, and torsion) for normal and non-abnormal distribution in repaired Fontan patients. Comparisons among 3 groups were made with one-way analysis of variance (ANOVA) for normally distributed data and the Kruskal-Wallis test for non-normally distributed continuous variables. According to the determined distribution, the Tukey's and Dunn's multiple comparisons tests as post hoc analysis were used in the comparative analysis between the 2 groups. Both intra-

observer and inter-observer variabilities were calculated as the mean difference and intra class correlation coefficient between 2 independently measured variables. Statistical significance was indicated by $P < 0.05$.

Results

Between August 2014 and January 2019, 32 (18 male, 14 female) Fontan patients underwent CMR. Of these 32 patients, 10 were excluded due to pulmonary hypertension in 4 cases, a morphologic right systemic ventricle in 4 cases, and poor image quality in 2 cases. For the final analysis, a total of 22 (15 male, 7 female, 10.09 ± 3.26 years) Fontan patients with morphological LV and 17 (10 male, 7 female, 11.23 ± 2.19 years) control subjects were included. Of the 22 Fontan patients, 10 had a single left ventricle (5 tricuspid atresia, 2 transpositions of the great artery, 3 others) and 12 had a dominant left ventricle (6 tricuspid atresia, 6 pulmonary atresias with an intact ventricular septum). With respect to NT-proBNP levels, 9/22 (41%) had elevated levels (>125 pg/mL) while 13/22 (59%) had normal levels (<125 pg/mL). Additional data for the Fontan patients, including operative procedure and New York Heart Association (NYHA) classification are summarized in *Table 1*.

Cardiac function

Basic cardiac function values in the Fontan patients and control subjects are summarized in *Table 2*. There were no significant differences between Fontan patients and control subjects for heart rate ($P=0.342$), EDVi ($P=0.704$), ESVi ($P=0.193$), SVi ($P=0.90$), EF ($P=0.05$), and COi ($P=0.221$).

Ventricular strain and torsion

Results of the strain and torsion analyses in the Fontan patients and control subjects are summarized in *Table 2*. The magnitude of GLS and GRS was significantly lower in Fontan patients than in control subjects ($P < 0.001$ for GLS; $P=0.002$ for GRS). GCS was similar in Fontan patients and control subjects ($P=0.235$). Peak systolic torsion and peak systolic torsion rates were significantly lower in Fontan patients than the control group ($P=0.044$, $P=0.017$, respectively). The mean peak systolic torsion of repaired Fontan patients was 0.66 ± 0.62 deg/cm, compared with 0.91 ± 0.42 deg/cm in the control group. The mean peak torsion rate of repaired Fontan patients was 4.22 ± 6.66 deg/(cm*s),

Table 2 CMR measurements in patients and controls

Baselines characteristics and CMR data	Fontan Patients		Control subjects (n=17)	P1	P2	P3	P4
	All (n=22)	NT-proBNP <125 pg/mL (n=13)					
Age at CMR (years)	10.09±3.26	10.92±3.66	11.23±2.19	0.199	0.155	0.021*	0.909
Sex (male/female)	15/7	10/3	10/7	-	-	-	-
Time since Fontan surgery (years)	6.00±2.33	6.31±2.42	NA	-	0.471	-	-
Heart rate (beats per minute)	81±16	82±19	77±14	0.342	0.81	0.499	0.391
Body surface area (m ²)	1.08±0.31	1.18±0.31	1.17±0.16	0.267	0.112	0.026*	0.871
EDV index (mL/m ²)	85.19±34.69	80.94±30.6	81.71±16.08	0.704	0.836	0.826	0.930
ESV index (mL/m ²)	35.32±16.63	34.39±16.86	29.72±5.73	0.193	0.961	0.318	0.294
Stroke volume index (mL/m ²)	50.00±21.22	46.85±17.73	50.74±12.91	0.90	0.721	0.846	0.492
EF (%)	59.38±6.61	59.54±7.50	63.36±4.77	0.05	0.892	0.052	0.100
Cardiac output index (L/min*m ²)	4.78±2.88	5.30±2.94	3.86±1.07	0.221	0.407	0.614	0.072
LV Cardiac mass index (mg)	51.24±16.60	50.29±16.87	69.06±17.21	0.002**	0.835	0.012**	0.006**
Left AV valve regurgitation (%)	17.34±8.65	17.05±4.07	-	-	0.917	-	-
GLS (%)	-15.19±2.94	-15.59±2.72	-19.97±1.70	<0.001***	0.462	<0.001***	<0.001***
GCS (%)	-16.76±3.27	-17.95±2.43	-17.88±2.26	0.235	0.036*	0.02*	0.934
GRS (%)	30.45±7.58	32.70±7.53	37.88±6.99	0.002**	0.095	<0.001***	0.047
Peak systolic torsion (deg/cm)	0.81±0.41	0.67±0.43	1.07±0.36	0.044*	0.036*	0.605	0.01*
Peak torsion rate (deg/cm*s)	7.36±3.41	6.72±3.21	9.85±2.61	0.017*	0.30	0.22	0.006**

*, P<0.05; **, P<0.01; ***, P<0.001. Data are reported as mean ± standard deviation. Bolded numbers represent differences of statistical significance. P1, all Fontan vs. control; P2, high NT-proBNP vs. normal NT-proBNP; P3, high NT-proBNP vs. control; P4, normal NT-proBNP vs. control. NA, not applicable.

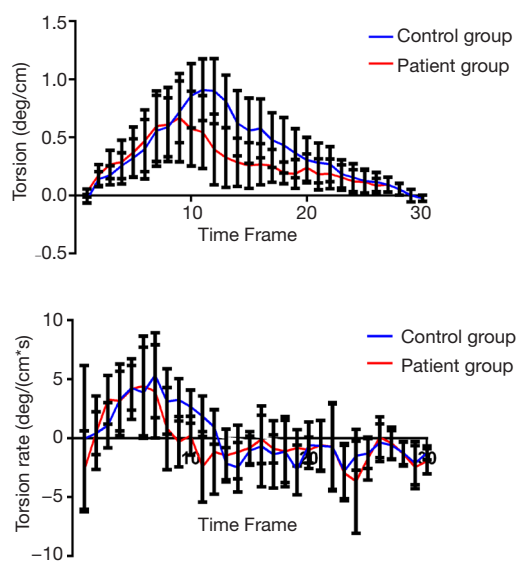


Figure 2 Comparison of average peak torsion and peak torsion rates between the repaired Fontan and control groups. The mean peak systolic torsion of repaired Fontan patients was 0.66 ± 0.62 deg/cm, compared with 0.91 ± 0.42 deg/cm in the control group. The mean peak torsion rate of repaired Fontan patients was 4.22 ± 6.66 deg/(cm*s), compared with 5.34 ± 5.66 deg/(cm*s) in the control group. The bar represents mean and SD 95% CI.

compared with 5.34 ± 5.66 deg/(cm*s) in the control group (Figure 2).

Correlation analysis with strain/torsion and NT-proBNP levels

GCS and torsion were strongly correlated with NT-proBNP in the patient group ($r=0.541$ for GCS; $r=0.588$ for torsion, $P<0.01$) (Table 3). The various volumetric and other parameters were not correlated with NT-proBNP in the patient group ($P>0.05$).

Subgroup analysis of Fontan patients with NT-proBNP levels

The results of the subanalysis of Fontan patients with normal and elevated NT-proBNP levels to each other and with control subjects are summarized in Table 2. The difference between GLS was significantly different among normal NT-proBNP levels (group 1), high NT-proBNP levels (group 2) in Fontan patients and the control group (group 3) ($P<0.001$). There was no significant difference

between the normal and high NT-proBNP level groups by multiple comparisons ($P>0.05$). GCS showed significant difference between the 3 groups ($P=0.0284$), and there was a statistical difference between group 1 and group 2, and group 2 and group 3 by multiple comparisons. GRS showed no significant difference between the 3 groups ($P=0.056$), but there was a difference between group 2 and group 3. Peak systolic torsion was significantly different among the normal and high NT-proBNP level groups in Fontan patients and the control group ($P<0.001$) (Figure 3), but there was no significant difference between the high NT-proBNP level group and the control group in multiple comparisons ($P>0.05$). Peak systolic torsion was significantly different among the 3 groups ($P=0.031$), and there was statistical difference in group 1 and group 2, and group 1 and group 3 by multiple comparisons (Figure 3). The peak torsion of the high NT-proBNP plasma level groups was higher than normal one in the patient group (1.01 ± 0.29 vs. 0.67 ± 0.43 , $P<0.05$).

Reproducibility

Table 3 summarizes the results of the intra-observer and inter-observer analysis for strain and torsion parameters. Intra-observer agreement was excellent for GLS, GCS, and GRS [all intraclass correlation coefficient (ICCs) $>92\%$] and acceptable for torsion (ICCs $>88\%$). Inter-observer agreement was lower than intra-observer agreement (all ICCs $>83\%$).

Discussion

Tissue tracking CMR can ascertain distinctive features of the myocardium throughout the cardiac cycle and calculate mechanical indices, such as strain, strain-rate, twist, and torsion. In our study, GLS and GRS were significantly lower in the repaired Fontan group compared with the control group. GLS is governed by sub-endocardial fibers, which run parallel to the long axis. GLS is susceptible to pathological processes that involve endocardial layers, and is one of the earliest markers of regional systolic dysfunction (13). There was compensation for cardiac muscle insufficiency in the repaired patient group, which made GLS continuing to decrease while GCS increase, lasting until GLS recovered (14). Our study found that cardiac function and GCS were not significantly different in the repaired Fontan group compared with the control group, while GLS was not significantly different in the

Table 3 Comparison of correlations between NT-proBNP, strain/torsion, and cardiac function in repair Fontan patients

NT-proBNP	r	P
EDV index (mL/m ²)	0.065	0.772
ESV index (mL/m ²)	0.08	0.716
Stroke volume index (mL/m ²)	0.04	0.851
EF (%)	-0.147	0.512
Cardiac output index (L/min*m ²)	-0.074	0.742
GLS (%)	0.247	0.267
GCS (%)	0.541*	0.009*
GRS (%)	-0.381	0.053
Peak systolic torsion (deg/cm)	0.588*	0.004*
Peak torsion rate (deg/cm*s)	0.029	0.895
EF (%)		
Peak systolic torsion (deg/cm)	-0.30	0.139
Peak torsion rate (deg/cm*s)	-0.13	0.431

*, numbers represent differences of statistical significance. Bolded numbers represent differences of statistical significance.

normal NT-proBNP level group compared to the high NT-proBNP level group (*Table 2*). We also found that the GCS of the normal NT-proBNP level group was significantly lower than the GCS of the high NT-proBNP level group. We speculate that the deterioration in NT-proBNP levels represents a repeated ventricular overload. Finally, GLS continued to decrease over time due to the failure of compensatory changes in GCS, myocardial pump failure, and ventricular dilation ensue.

GLS was found to be an independent and superior predictor of outcome when compared with radial and circumferential strain defined by late gadolinium enhancement (15). In our study, GLS differed significantly with normal and abnormal NT-proBNP levels and healthy controls. There was no significant difference between the normal and high NT-proBNP level groups by multiple comparisons. Meanwhile, GLS was not correlated with NT-proBNP in the patient group. But it was more correlated with serum biomarkers of ventricular function than ventricular size or ejection fraction ($r=0.247$ $P=0.267$) (*Table 3*). These results are in accordance with other findings that have GLS as an earlier marker of contractile dysfunction than GCS (16).

In our study, peak systolic torsion and peak systolic torsion rates were lower in the repaired Fontan group than the control group. There are explanations for this

finding. Firstly, cardiac microstructural changes could lead to reduced twisting. Fontan circulation results from the routing of the systemic venous blood to pulmonary circulation without a hydraulic source of a ventricle. Secondly, functional single ventricle (FSV) is often characterized by volume overload with resultant dilation, rearrangement of myofiber, and myocardial fibrosis in the early stage before operation (17). As myocardial fibrosis is more pronounced in the epicardium, it reduces the counter clock-wise motion dominated by a left-handed helix at the epicardium, and it is one of the reasons for the reduction of twisting in FSV (4). In our study, the average peak systolic torsion of repaired Fontan patients was 0.66 ± 0.62 deg/cm and occurred much earlier than with the 0.91 ± 0.42 deg/cm peak of the control group. The mean peak torsion rate of repaired Fontan patients was 4.22 ± 6.66 deg/(cm*s) [compared with 5.34 ± 5.66 deg/(cm*s) in the control group]. We found that the torsion and torsion rate peaked earlier than those of the control group (*Figure 2*). This can be explained by the following. First, the deterioration in twisting motion stemmed from the rearrangement of myofibers that could not be relieved in the Fontan patient group. Interestingly, the LV torsion rate and torsion rate did not demonstrate a significant relationship with LVEF in our study ($r=-0.30$, $P=0.139$ for torsion; $r=-0.17$, $P=0.43$ for torsion rate). This suggests that the LV torsion and torsion

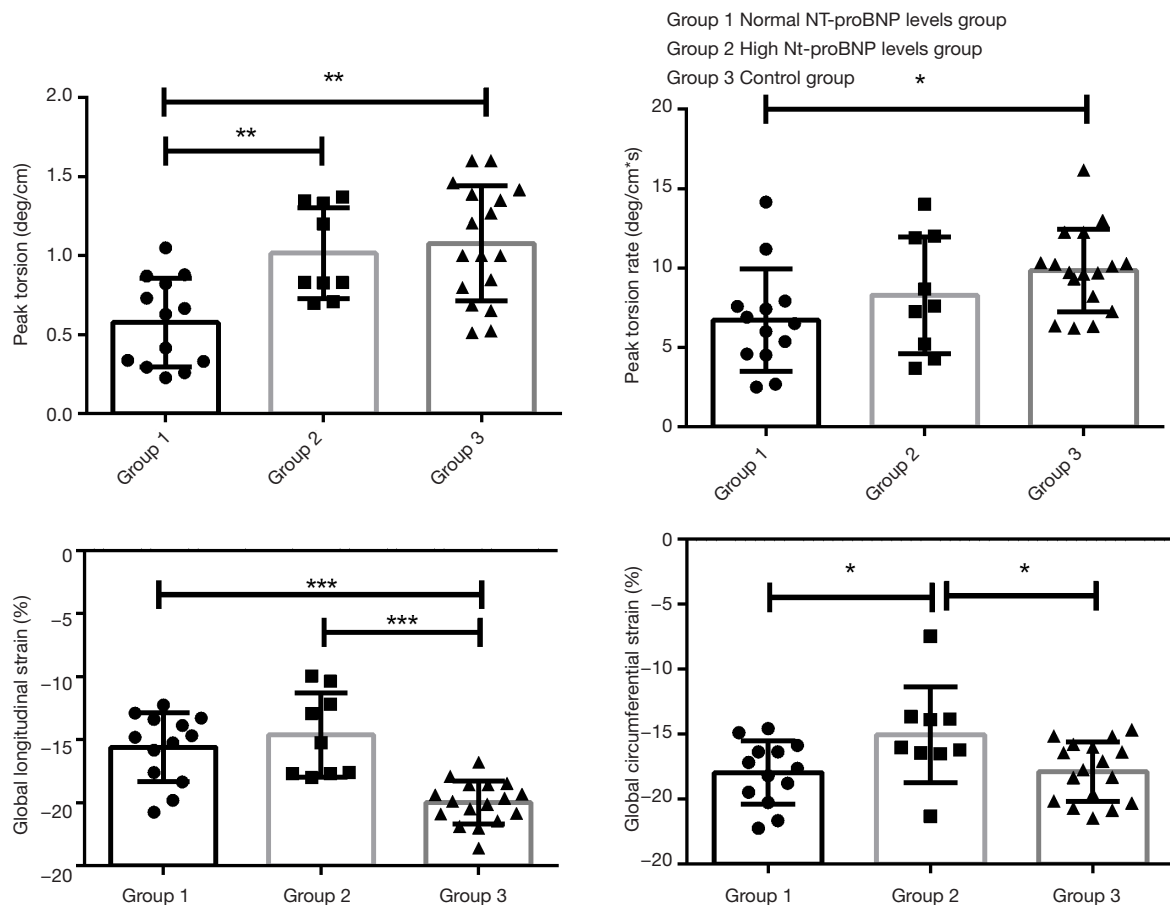


Figure 3 Comparison of cardiac strain and torsion stratified according to NT-proBNP levels (high >125 pg/mL and normal <125 pg/mL) in the repaired Fontan patients and healthy control groups. The difference between repaired Fontan patients with high NT-proBNP levels and healthy controls yielded significance for the peak torsion ($P < 0.05$). Longitudinal strains differed significantly between 3 groups. The box plot is the median and interquartile range for strain and torsion in patients and healthy controls. Group 1: repaired Fontan patients with normal NT-proBNP levels. Group 2: repaired Fontan patients with abnormal NT-proBNP levels. Group 3: healthy controls. *, $P < 0.05$; **, $P < 0.01$; ***, $P < 0.001$.

rate may be reduced earlier in post-Fontan cases compared with controls when the LV function is preserved. Second, the anatomical abnormality of FSV also contributes to an imbalanced twisting motion. In contrast to an LV in the normal heart, the suboptimal ventricular function of FSV may result in a poor twisting motion, leading to an earlier peak systolic torsion. As torsion contributes to energy-efficient ejection, reduced torsion might be a potential marker for early myocardial dysfunction (18). However, this hypothesis requires further prospective evaluation.

Previous research reported (19,20) increased apical twist in severe LV pressure overload and aortic stenosis, which occurred as an adaptive or compensatory mechanism. Gnakamene *et al.* (21) showed that basal LV torsion was

associated with increased aortic stiffness and improved diastolic function with hypertension. In our study, the difference between repaired Fontan patients with normal NT-proBNP levels and healthy controls yielded significance for the peak torsion. The reason for this is that low preload with chronic myocardial remodeling after the Fontan operation leads to altered ventricular geometry, decreased compliance, increased end-diastolic pressure, and possible high NT-proBNP plasma levels (1). In our study, LV function, cardiac mass, and AV valve regurgitation were not statistically different between the normal NT-proBNP level and high NT-proBNP level subjects.

Meanwhile, peak systolic torsion was significantly lower in Fontan patients with normal NT-proBNP level than in

Table 4 Intra-observer and inter-observer variability for strain and torsion indices

Parameter	Intra-observer (n=20)		Inter-observer (n=20)	
	Biases \pm SD	ICC	Biases \pm SD	ICC
GLS (%)	0.04 \pm 3.26	98.4%	0.32 \pm 3.36	96%
GCS (%)	0.66 \pm 2.34	95.7%	0.85 \pm 2.59	89.1%
GRS (%)	1.03 \pm 7.67	92.4%	1.52 \pm 6.65	86.8%
Peak torsion (deg/cm)	0.04 \pm 0.39	90.7%	0.18 \pm 0.36	83.5%
Peak torsion rate (deg/cm*s)	0.12 \pm 2.24	88.5%	0.17 \pm 2.41	85.7%

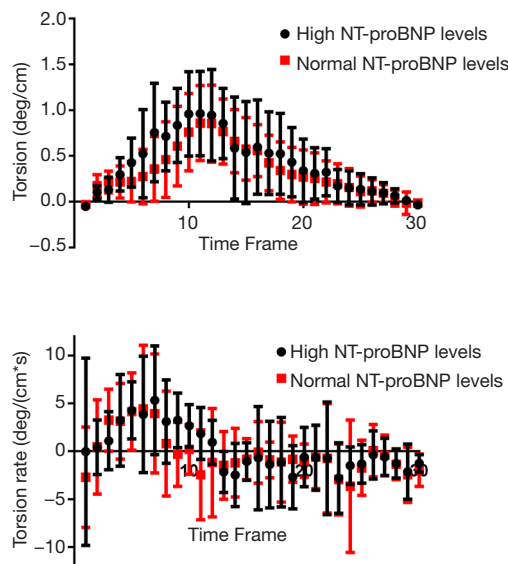


Figure 4 Comparison of torsion and torsion rate stratified according to NT-proBNP levels with all phases (high >125 pg/mL and normal <125 pg/mL) in the repaired Fontan patients. The bar is mean and SD 95% CI.

high NT-proBNP level subjects (Figure 4). Our explanation for this is that the high NT-proBNP level subjects entered the compensatory period (elevated afterload) earlier than the normal NT-proBNP level subjects. Twisting helps generate high ventricular pressure and a large ventricular ejection volume, with the highest cardiac working efficiency.

Furthermore, torsion was strongly correlated with NT-proBNP in the patient group ($r=0.588$ for torsion, $P<0.01$). Torsion may be a key factor of a compensatory mechanism to maintain global systolic function during following up of Fontan patients, despite the alteration of myocardial shortening and structure. Although LV torsion has not yet been included in clinical practice guidelines, its

inclusion will likely prove to be useful (7).

NT-proBNP is the best independent predictor of mortality, and was shown to be able to assess mortality risk for all patients in a large cohort comprising every CHD type (22). Our study excluded abnormalities in glomerular filtration rate, pulmonary hypertension, and valvular stenosis, and we ensured that the NT-proBNP plasma level was not affected by the influence of obesity and renal function. The repaired Fontan patients were NYHA I–II in our study; which does not warrant a positive long-term clinical outcome in contrast to low values of NT-proBNP (Table 1). In our study, 3 cases had reduced EF (<55%), but 8 cases had significantly elevated NT-proBNP plasma levels (>125 pg/mL). High NT-proBNP plasma levels are associated with the severity of ventricular systolic dysfunction. NT-proBNP is the standard of decompensation for cardiac insufficiency and represents an increase of ventricular pressure. The increase of ventricular pressure is the main reason for the increase of NT-proBNP, while there is no relationship between EF and NT-proBNP (23). Meanwhile, the parameters of cardiac function were not correlated with NT-proBNP in the patient group (Table 3).

Biases and ICC for global strain, torsion, and torsion rates for intra-observer and inter-observer variability are summarized in Table 4. GLS showed a higher ICC (0.98 and 0.96) than GCS and GRS. There was good reproducibility for global peak torsion (ICC 0.90 and 0.83) and global peak systolic torsion rate (ICC 0.88 and 0.85).

Limitations

There are some limitations to this study. Firstly, this was a single-center, retrospective study performed at a large hospital, so the inherent limitations of this study design cannot be avoided. The number of volunteers in the control group was also limited. Secondly, some authors

mentioned that NT-proBNP is affected by body-mass index, age, and the sex of patients, and we did not evaluate the impact of these co-variables in this study (24). Thirdly, late enhancement was only performed in some post-Fontan cases, so the clinical utility of the late myocardial enhancement should be investigated in future studies. Fourthly, some investigators have also expressed torsion as representing the shear deformation angle, with torsion normalized by twist angle and LV radius; we did not assess the torsional shear angle in our study.

Meanwhile, GRS is not a good indicator of repeatability in strain research, so its clinical significance is extremely limited. We also did not discuss the value of GRS (25). Fifth, myocardial strain and torsion of the single ventricle with the dominant left ventricle were analyzed in Fontan patients. There were 10 cases of single ventricle with the dominant left ventricle and 12 cases of complex 2 ventricles (the functional single left ventricle with hypoplastic right ventricle; the hypoplastic right ventricle was not included in strain and torsion analysis. In the exclusion criteria of our study, a single ventricle with dominant morphological RV was excluded because of the difference in RV and LV mechanics. The ventricular mechanics in Fontan patients with single ventricles have rarely been studied, and it remains uncertain how the mechanical changes of single ventricle with dominant left ventricle differs from those of functional single left ventricle with hypoplastic right ventricle in the repaired Fontan patients. This mechanism needs to be further studied and confirmed. Sixth, the regional strain may better explain the myocardial strain in a compensatory period than global strain, and it should be investigated in future studies.

Conclusions

Strain and peak systolic torsion analysis, as measured by CMR, are clinically feasible and accessible tools for systemic ventricular function quantification. GLS is an earlier marker of contractile dysfunction in repair Fontan patients. Peak systolic torsion may be a biomarker for determining subclinical dysfunction, as it is more strongly correlated with serum biomarkers of ventricular function than ventricular size or ejection fraction.

Acknowledgments

Funding: The present study was funded by the National Key Research and Development Program (No. 2018YFB110710,

to YM Zhong), the Shanghai Committee of Science and Technology (No. 17DZ2253100, to LW Hu), the Shanghai Municipal Commission of Health and Family Planning (No. 20164Y0150, to LW Hu), and the Shanghai “Rising Stars of Medical Talent” Medical Imaging Practitioner Program (to LW Hu).

Footnote

Conflicts of Interest: The authors have no conflicts of interest to declare.

Ethical Statement: The study was approved by the Institutional Review Board and written informed consent was obtained from all patients.

References

1. Sabanayagam A, Cavus O, Williams J, Bradley E. Management of Heart Failure in Adult Congenital Heart Disease. *Heart Fail Clin* 2018;14:569-77.
2. Ponikowski P, Voors AA, Anker SD, Bueno H, Cleland JGF, Coats AJS, Falk V, González-Juanatey JR, Harjola VP, Jankowska EA, Jessup M, Linde C, Nihoyannopoulos P, Parissis JT, Pieske B, Riley JP, Rosano GMC, Ruilope LM, Ruschitzka F, Rutten FH, van der Meer P. 2016 ESC Guidelines for the Diagnosis and Treatment of Acute and Chronic Heart Failure. *Rev Esp Cardiol (Engl Ed)* 2016;69:1167.
3. Torrent-Guasp F, Kocica MJ, Corno AF, Komeda M, Carreras-Costa F, Flotats A, Cosin-Aguillar J, Wen H. Towards new understanding of the heart structure and function. *Eur J Cardiothorac Surg* 2005;27:191-201.
4. Schuster A, Hor KN, Kowallick JT, Beerbaum P, Kutty S. Cardiovascular Magnetic Resonance Myocardial Feature Tracking: Concepts and Clinical Applications. *Circ Cardiovasc Imaging* 2016;9:e004077.
5. Lamata P, Hussain ST, Kutty S, Steinmetz M, Sohns JM, Fasshauer M, Staab W, Unterberg-Buchwald C, Lotz J, Schuster A. Cardiovascular magnetic resonance myocardial feature tracking for the measurement of myocardial twist and untwist at rest and during dobutamine stress in healthy volunteers. *J Cardiovasc Magn Reson* 2014;16:14.
6. Truong UT, Li X, Broberg CS, Houle H, Schaal M, Ashraf M, Kilner P, Sheehan FH, Sable CA, Ge S, Sahn DJ. Significance of mechanical alterations in single ventricle patients on twisting and circumferential strain as determined by analysis of strain from gradient cine

- magnetic resonance imaging sequences. *Am J Cardiol* 2010;105:1465-9.
7. Sengupta PP, Tajik AJ, Chandrasekaran K, Khandheria BK. Twist mechanics of the left ventricle: principles and application. *JACC Cardiovasc Imaging* 2008;1:366-76.
 8. Carreras F, Garcia-Barnes J, Gil D, Pujadas S, Li CH, Suarez-Arias R, Leta R, Alomar X, Ballester M, Pons-Llado G. Left ventricular torsion and longitudinal shortening: two fundamental components of myocardial mechanics assessed by tagged cine-MRI in normal subjects. *Int J Cardiovasc Imaging* 2012;28:273-84.
 9. Poveda F, Gil D, Martí E, Andaluz A, Ballester M, Carreras F. Helical structure of the cardiac ventricular anatomy assessed by diffusion tensor magnetic resonance imaging with multiresolution tractography. *Rev Esp Cardiol (Engl Ed)* 2013;66:782-90.
 10. Yoneyama K, Venkatesh BA, Wu CO, Mewton N, Gjesdal O, Kishi S, McClelland RL, Bluemke DA, Lima JAC. Diabetes mellitus and insulin resistance associate with left ventricular shape and torsion by cardiovascular magnetic resonance imaging in asymptomatic individuals from the multi-ethnic study of atherosclerosis. *J Cardiovasc Magn Reson* 2018;20:53.
 11. Redfield MM, Rodeheffer RJ, Jacobsen SJ, Mahoney DW, Bailey KR, Burnett JC Jr. Plasma brain natriuretic peptide concentration: impact of age and gender. *J Am Coll Cardiol* 2002;40:976-82.
 12. Suever JD, Wehner GJ, Jing L, Powell DK, Hamlet SM, Grabau JD, Mojsejenko D, Andres KN, Haggerty CM, Fornwalt BK. Right Ventricular Strain, Torsion, and Dyssynchrony in Healthy Subjects using 3D Spiral Cine DENSE Magnetic Resonance Imaging. *IEEE Trans Med Imaging* 2017;36:1076-85.
 13. Deal BJ, Jacobs ML. Management of the failing Fontan circulation. *Heart* 2012;98:1098-104.
 14. Hu L, Sun A, Guo C, Ouyang R, Wang Q, Yao X, Zhong Y. Assessment of global and regional strain left ventricular in patients with preserved ejection fraction after Fontan operation using a tissue tracking technique. *Int J Cardiovasc Imaging* 2019;35:153-60.
 15. Hor KN, Gottlieb WM, Carson C, Wash E, Cnota J, Fleck R, Wansapura J, Klimeczek P, Al-Khalidi HR, Chung ES, Benson DW, Mazur W. Comparison of magnetic resonance feature tracking for strain calculation with harmonic phase imaging analysis. *JACC Cardiovasc Imaging* 2010;3:144-51.
 16. Ishizaki U, Nagao M, Shiina Y, Inai K, Mori H, Takahashi T, Sakai S. Global strain and dyssynchrony of the single ventricle predict adverse cardiac events after the Fontan procedure: Analysis using feature-tracking cine magnetic resonance imaging. *J Cardiol* 2019;73:163-70.
 17. Zhong SW, Zhang YQ, Chen LJ, Wang SS, Li WH, Sun YJ. Ventricular Twisting and Dyssynchrony in Children with Single Left Ventricle Using Three-Dimensional Speckle Tracking Imaging after the Fontan Operation. *Echocardiography* 2016;33:606-17.
 18. Binotto MA, Higuchi Mde L, Aiello VD. Left ventricular remodeling in hearts with tricuspid atresia: morphologic observations and basis for ventricular dysfunction after surgery. *J Thorac Cardiovasc Surg* 2003;126:1026-32.
 19. Young AA. Ventricular Torsion: An Aid to Ejection? *JACC Cardiovasc Imaging* 2012;5:282-4.
 20. Rüssel IK, Götte MJ, Bronzwaer JG, Knaapen P, Paulus WJ, van Rossum AC. Left Ventricular Torsion: An Expanding Role in the Analysis of Myocardial Dysfunction. *JACC Cardiovasc Imaging* 2009;2:648-55.
 21. Gnakamene JB, Safar ME, Levy BI, Escoubet B. Left Ventricular Torsion Associated with Aortic Stiffness in Hypertension. *J Am Heart Assoc* 2018. doi: 10.1161/JAHA.117.007427.
 22. Sengupta PP, Narula J. Cardiac Strain as a Universal Biomarker: Interpreting the Sounds of Uneasy Heart Muscle Cells. *JACC Cardiovasc Imaging* 2014;7:534-6.
 23. Popelová JR, Kotaška K, Tomková M, Tomek J. Usefulness of N-Terminal pro-brain natriuretic peptide to predict mortality in adults with congenital heart disease. *Am J Cardiol* 2015;116:1425-30.
 24. Tsutamoto T, Wada A, Sakai H, Ishikawa C, Tanaka T, Hayashi M, Fujii M, Yamamoto T, Dohke T, Ohnishi M, Takashima H, Kinoshita M, Horie M. Relationship between renal function and plasma brain natriuretic peptide in patients with heart failure. *J Am Coll Cardiol* 2006;47:582-6.
 25. Aurich M, Keller M, Greiner S, Steen H, Aus dem Siepen F, Riffel J, Katus HA, Buss SJ, Mereles D. Left ventricular mechanics assessed by two-dimensional echocardiography and cardiac magnetic resonance imaging: comparison of high-resolution speckle tracking and feature tracking. *Eur Heart J Cardiovasc Imaging* 2016;17:1370-8.

Cite this article as: Hu LW, Liu XR, Wang Q, Barton GP, Ouyang RZ, Sun AM, Guo C, Han TT, Yao XF, François CJ, Zhong YM. Systemic ventricular strain and torsion are predictive of elevated serum NT-proBNP in Fontan patients: a magnetic resonance study. *Quant Imaging Med Surg* 2020;10(2):485-495. doi: 10.21037/qims.2020.01.07